

United States
Department of
Agriculture

Natural Resources
Conservation
Service

11 Campus Boulevard
Suite 200
Newtown Square, PA 19073

Subject: Soils – Ground-Penetrating Radar (GPR) Field Assistance

Date: 15 November 2000

To: Dr. Robert Graham
Professor of Soil Mineralogy
Department of Soils & Environmental Sciences
2208 Geology Building
University of California, Riverside, CA 92521-0424

Purpose:

The purpose of this investigation was to measure depths to unweathered or weakly weathered granitic bedrock (R layers) with GPR in the Sierra Nevada Range of Tulare County, California.

Participants:

Jim Doolittle, Research Soil Scientist, USDA-NRCS, Newtown Square, PA
Bob Graham, Professor of Soil Mineralogy, Department of Soils & Environmental Sciences, University of California, Riverside, CA
Sam Indorante, MLRA Project Leader, USDA-NRCS, Carbondale, IL
James Witty, Graduate Student, Department of Soils & Environmental Sciences, University of California, Riverside, CA

Activities:

All activities were completed during the period of 10 to 15 October 2000.

Background:

In many west slope areas of the Sierra Nevada Range of California, soil and climatic conditions are relatively harsh for plants. The soil moisture regime is xeric with a pronounced and severe summer dry season. Extensive areas are underlain by coarse- and moderately coarse-textured soils that are shallow (0-50 cm) and moderately deep (50 to 100 cm) over granitic bedrock. These soils have very low available water capacities. Despite these harsh conditions, the biomass within the Chaparral and mixed coniferous ecosystems is considered extraordinary (Jones and Graham, 1993).

In the Sierra Nevada Range, the granitic bedrock is typically highly weathered in the upper part. Weathered bedrock (Cr material) can hold a substantial amount of plant-available water (Jones and Graham, 1993; Anderson et al., 1995). In some areas, the amount of plant-available water is greater in the weathered bedrock than in the overlying soil. Though root restrictive, Cr materials can contain a substantial amount of plant-available water especially along fractures and joints (Jones and Graham, 1993; Anderson et al., 1995). In Southern California, roots have been observed at depths as great as 8.5 m within the rock substrate (Jones and Graham, 1993). The thickness, structure, texture, weathering and fracturing qualities of Cr materials are highly variable. The Cr materials grades with depth into hard, weakly weathered or unweathered bedrock.

The purpose of this investigation was to use ground-penetrating radar to measure depths to weakly weathered or unweathered rock (R layers). These materials correspond to Clayton and Arnold's (1972) weathering classes 1 to 3. They cannot be augered through with hand augers and produce a strong and identifiable "ring" when struck with a metallic object. Within each study site, depths to Cr material have been measured with soil augers. The Cr material corresponds to Clayton and Arnold's (1972) weathering classes 4 through 7. Ground-penetrating radar depth interpretations will be used to associate the growth of ponderosa pine (*Pinus ponderosa*) trees with the depth and thickness of Cr materials and the depth to R layers.

Ground-penetrating radar can provide high-resolution mapping of the depths to bedrock (Davis and Annan, 1989; Morey, 1974; Olson and Doolittle, 1985). Collins and others (1989) found GPR to be more rapid, economical, and reliable than conventional auger techniques for determining the depth to bedrock and the composition of soil map units based on soil-depth criteria. However, GPR is not equally suited to all soils (Doolittle, 1987) or rock types (Rubin and Fowler, 1978).

Where terrain conditions are appropriate, GPR is an excellent tool to map bedrock depths and show soil-bedrock relationships (Schellentrager and Doolittle, 1991; Doolittle et al., 1988; Collins et al., 1989; Collins et al., 1990 and 1994; Puckett et al., 1990). Ground-penetrating radar is sensitive to changes in rock types and fractures (Davis and Annan, 1989). Ground-penetrating radar has been used to detect low-dipping fractures or dikes in bedrock (Davis and Annan, 1989; Holloway and Mugford, 1990, Stevens et al., 1995). In areas underlain by different lithologies, GPR has been used to identify and characterize changes in rock types (Benson and Yuhr, 1992; Bjelm et al., 1983, Robillard et al., 1994; Sigurdsson, 1994). This application has been most successful in areas where the underlying lithologies have strongly contrasting electrical properties or internal structure.

In areas underlain by weathered bedrock, the electrical properties of weathered rock are often similar to those of the overlying residual soils and the underlying unweathered bedrock. In these areas it is difficult to identify the soil/bedrock interface or to differentiated weathered rock from unweathered rock. However, with experience, these reflectors can be recognized on most radar profiles with little ambiguity. Robillard and others (1994) observed that the surface of unweathered bedrock often appears as a continuous reflector of variable amplitude. These researchers associated variations in the amplitude of the reflected signal with differences in rock hardness and mineralogy. Leggo and others (1992) used GPR techniques to distinguish variations in the degree of argillization in granitic bedrock. Robillard and others (1994) observed corestones within more highly weathered bedrock matrix.

Equipment:

The radar unit is the Subsurface Interface Radar (SIR) System-2000, manufactured by Geophysical Survey Systems, Inc.¹ Morey (1974), Doolittle (1987), and Daniels (1996) have discussed the use and operation of GPR. The SIR System-2000 consists of a digital control unit (DC-2) with keypad, VGA video screen, and connector panel. A 12-volt battery powered the system. This unit is backpack portable and, with an antenna, requires two people to operate. The antennas used in this study were the 200 MHz and 400 MHz. Scanning times were either 120 or 160 nanoseconds (ns). Hard copies of the radar data were printed in the field on a model T-104 printer.

Study Sites:

Radar traverses were conducted at sites located in the Sequoia National Forest in eastern Tulare County, California. All sites are forested. Soils formed principally in residuum weathered from granite bedrock. Chemical weathering has decomposed the upper part of the bedrock and relatively thick layers of Cr material are present. These layers vary in degree of chemical alteration, fracturing, and mechanical strength. Principal soils that have been mapped within the general area are Chaix and Chawanakee. Chaix soils are members of the coarse-loamy, mixed, mesic Dystric Xerochrepts family. Chawanakee soils are members of the loamy, mixed, mesic, shallow Dystric Xerochrepts family. The well drained to somewhat excessively drained Chaix soils are moderately deep over highly weathered bedrock. The somewhat excessively drained Chawanakee soils are shallow over highly weathered bedrock. Both soils have a low available water capacity. At the time of this investigation, a thin (0 to 2 in) snow cover mantled most sites.

Field Procedures:

At each site, a traverse line was established around a dominant ponderosa pine tree. These lines completely or partially encircled the tree or consisted of parallel lines located on either side of the tree. Lines were of variable lengths and spaced about 2 to 5 meters away from the tree. Vegetation and debris were removed from the traverse lines. Survey flags were inserted in the ground at intervals of about 1 meter along each traverse line and served as observation points. Radar surveys were completed by pulling the 200 MHz antenna along these traverse lines. As the radar antenna was pulled passed each observation point, the operator impressed a vertical mark on the radar record. The radar profiles were reviewed in the field and printed each night. Later the Cr/R interface was interpreted and the depth to the R material measured at each observation point. All radar profiles have been stored on disc. Table 1 summarizes the traverse data.

CALIBRATION OF GPR

Ground-penetrating radar is a time scaled system. This system measures the time it takes electromagnetic energy to travel from an antenna to an interface (i.e., soil horizon, bedrock surface, lithologic layer) and back. To convert travel time to depth requires knowledge of the velocity of pulse propagation. Several methods are available to determine the velocity of propagation. These methods include use of table values, common midpoint calibration, and calibration over a target of known depth. The last method is considered the most direct and accurate method to estimate propagation velocity. The procedure involves measuring the two-way

¹ Manufacturer's names are provided for specific information; use does not constitute endorsement.

| File # | Tree # | Points | Geometry | Time (ns) | Antenna |
|--------|--------|--------|-------------|-----------|---------|
| 13 | 1 | 23 | full circle | 160 | 200 |
| 14 | 6 | 26 | full circle | 160 | 200 |
| 15 | 7 | 12 | full circle | 160 | 200 |
| 16 | 34 | 23 | full circle | 160 | 200 |
| 17 | 3 | 26 | full circle | 160 | 200 |
| 18 | 5 | 23 | full circle | 120 | 200 |
| 19 | 32 | 16 | half circle | 120 | 200 |
| 20 | 33 | 27 | full circle | 120 | 200 |
| 21 | 4 | 29 | full circle | 120 | 200 |
| 22 | 8 | 19 | half circle | 120 | 200 |
| 23 | 30 | 26 | full circle | 120 | 200 |
| 24 | 31 | 29 | full circle | 120 | 200 |
| 25 | 29 | 31 | full circle | 120 | 200 |
| 26 | 17 | 27 | full circle | 120 | 200 |
| 27 | 25&24 | 31 | full circle | 120 | 200 |
| 28 | 26 | 14 | two lines | 120 | 200 |
| 29 | 27&28 | 13&10 | two lines | 120 | 200 |
| 30 | 27&28 | 13&10 | two lines | 120 | 200 |
| 31 | 15 | 29 | full circle | 120 | 200 |
| 32 | 14 | 25 | full circle | 120 | 200 |
| 33 | 14 | 25 | full circle | 160 | 200 |
| 34 | 13 | 31 | full circle | 160 | 200 |
| 35 | 21 | 25 | full circle | 160 | 200 |
| 36 | 20 | 19 | half circle | 160 | 200 |
| 37 | 22 | 14 | half circle | 160 | 200 |
| 38 | 23 | 14 | half circle | 160 | 200 |

Table 1 – Summary of Transects. The sequential file numbers refer to the recorded radar files and should be used to identify radar transects. The tree number identifies the tree. Points refer to the number of observation point on traverse line(s). Time refers to the two-way travel time used on the GPR.

travel time to a known reflector on the radar profile and calculating the propagation velocity by following equation (after Morey, 1974):

$$V = 2D/T \quad [1]$$

Equation [1] describes the relationship of the average propagation velocity (V) to the depth (D) and two-way pulse travel time (T) to a reflector. During the course of this investigation, depths to soil or bedrock interfaces were made at six holes excavated with a soil auger. At each observation point, the measured depth (D) and the two-way radar pulse travel time to a recognized subsurface interface were used to estimate the velocity of propagation. Measured depth to the six subsurface interfaces ranged from 0.51 to 2.9 meters. The estimated velocity of propagation determined to each of these interfaces is shown in Table 2.

| Feature | Depth | Time | Velocity | Er |
|---------|-------|-------|----------|-----|
| Shovel | 0.51 | 7.00 | 0.15 | 4.3 |
| Cr | 1.91 | 17.80 | 0.21 | 2.0 |
| R | 0.89 | 11.80 | 0.15 | 4.0 |
| R | 1.60 | 16.80 | 0.19 | 2.5 |
| R | 2.90 | 35.00 | 0.17 | 3.3 |
| R | 2.26 | 21.70 | 0.21 | 2.1 |

Table 2 – Estimated Velocities of Propagation. Estimates were determined using the two-way travel time to subsurface interface reflections that appeared on radar profiles, the measured depths to the interface, and equation [1]. Depths are expressed in meters. Time is expressed in ns. Velocity is expressed in m/ns.

The velocity of propagation is both temporally and spatially variable. Temporal variations are attributed to snowmelt, rainfall, and throughflow events that influence soil moisture contents. Lateral and vertical variations in propagation velocity occur as a result of changes in soil and lithologic properties. Within the study sites, the velocity of propagation increases with depth and principally reflects increased bulk densities and soil water contents. The estimated velocity of propagation ranged from 0.15 m/ns to 0.21 m/ns. The estimated dielectric permittivity ranged from 4.3 for surface layers to 2 to 3.3 for Cr materials. Because of this variability it would be difficult to accurately predict depths to subsurface interfaces across sites using a single or mean velocity of propagation.

Because of the variability in propagation velocities with increasing depth, a predictive equation, based on measured depths and two-way travel times to known subsurface interfaces, was used. The measured depth and the two-way travel time to the subsurface interfaces at the six observation points were compared. A strong ($r = 0.961$) and significant (0.001 level) relationship was found to exist between the two-way travel time of the radar pulse and the measured depth to these interfaces.

A least square line was fitted to the data and used to predict the depth to R layers at all observation points. The relationship is expressed as:

$$D = 0.06 + (0.088 * T) \quad [2]$$

Where D is depth in meters and T is the two-way travel time in nanoseconds to the interface.

For the five observed subsurface interfaces, using predictive equation [2], the average difference between the measured and the predicted depth was 0.21 m with a range of -0.24 to 0.29 m (see Table 3).

| Measured | Interpreted | Residual |
|----------|-------------|----------|
| 0.51 | 0.68 | -0.17 |
| 1.91 | 1.63 | 0.28 |
| 0.89 | 1.10 | -0.21 |
| 1.60 | 1.54 | 0.06 |
| 2.90 | 3.14 | -0.24 |
| 2.26 | 1.97 | 0.29 |

Table 3 - Comparison of Measured and Interpreted Depths to Subsurface Interfaces. Interpreted depths were determined using the two-way travel times to the identified subsurface interface reflection that appeared on radar profiles and predictive equation [2]. Depths are expressed in meters. Time is expressed in ns.

Interpretations:

Figure 1 is a representative radar profile from this study. This radar profile has been processed through the WINRAD software package. Processing was limited to signal stacking, distance normalization, color transforms and table customizing. Signal stacking, color transformation and table customization were used to reduce background noise and signal amplitudes.

In Figure 1, the parallel, multiple reflections at the top of the radar profile represent the soil surface. The horizontal scale represents units of distance traveled along the traverse line. The twenty-one white vertical lines at the top of the radar profile represent equally spaced observation points. These points are spaced at an interval of about 1 m. The vertical scale along the left-hand border of Figure 1 is a time scale. The scanning time used in this traverse was 160 ns. In Figure 1, using equation [2] and a scanning time of 160 ns, the maximum depth of penetration is about 14 m. However, signal quality deteriorates rapidly below a depth of about 120 ns and the maximum observation depth is less than 10.5 m. Depths to any subsurface interface can be estimated using the two-way travel time to the interface and equation [2].

In Figure 1, the Cr and R surfaces have been interpreted and identified with dark lines. Both surfaces form continuous reflectors that vary laterally in amplitude. The Cr provided a comparatively shallow, high amplitude reflection that was easily identified on most radar profiles. In Figure 1, depth to the Cr material ranges from about 0.5 to 1.2 m.

The identification of the R material was more challenging and interpretative. Auger borings confirmed the presence of multiple layers within the Cr material that differed in hardness and density. These layers produced unwanted reflections on radar profiles. The presence of intrusive materials (dikes), core stones, fractures, and sheeting within the granitic materials complicated and confused interpretations of the Cr/R contact. Core stones produced multiple, hyperbolic reflections. These reflections frequently interfered with and partially masked reflections from the Cr/R interface. Fractures often produced narrow, steeply inclined to vertical zones of multiple high amplitude reflections. Typically, fracture zones have higher moisture and clay contents than the

surrounding rock mass. Consequently, these features contrast with the surrounding rock mass and produce strong radar reflections. In Figure 1, several high amplitude planar reflectors have been identified. These reflectors are believed to represent either core stones (C), or fractures (F).

The identification and delineation of the R layer's upper surface was complicated by the occurrence of multiple planar reflectors within the bedrock. Because of the presence of these *unwanted layers* and *reflections*, the identification of the R layer was *more interpretative* and subject to error than desired. At most sites, a relatively smooth, continuous reflector of strong to moderate amplitude was chosen, traced laterally, and identified as the R layer. In Figure 1, the upper surface of the R layer has been identified. In this profile, the depth to the R layer ranges from about 3.0 to 6.4 m.

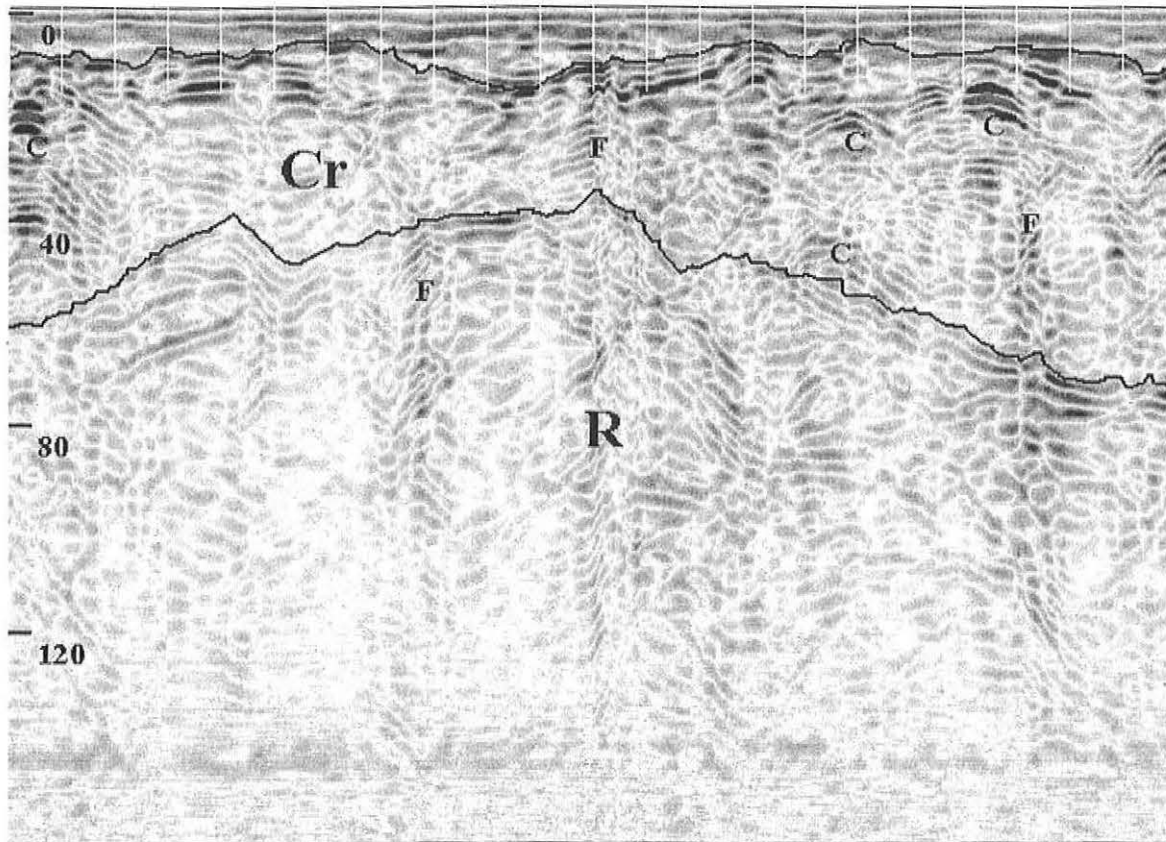


Figure 1 – Representative Radar Profile. Vertical scale is a time scale and is expressed in ns. The horizontal scale is in m.

Results:

The attached compendium summarizes the results of this investigation. Data from the last site has been omitted. Soils at this site had higher clay and moisture contents, an argillic horizon, and were developed in alluvial materials.

Data are arranged by radar file number (see Table 1 for tree number). The measured distance to the interpreted Cr/R interface was scaled (see scale column) converted into a two way travel time in nanoseconds (see time column) at each observation point. At each observation point, the depth (in meters) to Cr/R interface was determined using predictive equation [2] and the two-way travel time. An average depth to the R material has been included with each file.

It was my pleasure to assist and work with you again.

With kind regards,

James A. Doolittle
Research Soil Scientist

cc:

B. Ahrens, Director, USDA-NRCS, National Soil Survey Center, Federal Building, Room 152, 100 Centennial Mall North, Lincoln, NE 68508-3866
 C. Olson, National Leader, Soil Investigation Staff, USDA-NRCS, National Soil Survey Center, Federal Building, Room 152, 100 Centennial Mall North, Lincoln, NE 68508-3866
 H. Smith, Director of Soils Survey Division, USDA-NRCS, Room 4250 South Building, 14th & Independence Ave. SW, Washington, DC 20250
 E. Vinson, State Soil Scientist/MO Leader, NRCS, 2121-C 2nd Street, Davis, CA 95616

References:

- Anderson, M. A., R. C. Graham, G. J. Alyanakian, and D. Z. Martynn. 1995. Late summer water status of soils and weathered bedrock in a giant sequoia grove. *Soil Science* 160(6):415-422.
- Benson, R. and L. Yuhr. 1992. Assessment of bauxite reserves using ground penetrating radar. p. 229-236. IN: P. Hanninen and S. Autio (eds.) *Fourth International Conference on Ground-Penetrating Radar*. 7 to 12 June 1992. Rovaniemi, Finland. Geological Survey of Finland, Special Paper 16. pp. 365.
- Bjelm, L., S. Folin, and C. Svensson. 1983. A radar in geological subsurface investigation. *Bulletin of the International Association of Engineering Geology*. 26-27:10-14.
- Clayton, J. L., and J. F. Arnold. 1972. Practical grain size, fracturing density and weathering classification of intrusive rocks in the Idaho batholith. USDA Forest Service General Technical Report INT-2 Intermountain Forest Range Experiment Station, Ogden, Utah. p. 17.
- Collins, M. E., J. A. Doolittle, and R. V. Rourke. 1989. Mapping depth to bedrock on a glaciated landscape with ground-penetrating radar. *Soil Sci. Soc. Am. J.* 53: 1806-1812.
- Collins, M. E., W. E. Puckett, G. W. Schellentrager, and N. A. Yust. 1990. Using GPR for micro-analyses of soils and karst features on the Chiefland Limestone Plain in Florida. *Geoderma* 47:159-170.
- Collins, M. E., M. Crum, and P. Hanninen. 1994. Using ground-penetrating radar to investigate a subsurface karst landscape in north-central Florida. *Geoderma* 61:1-15.
- Daniels, D. J. 1996. *Surface-Penetrating Radar*. The Institute of Electrical Engineers, London, United Kingdom. 300 p.
- Davis, J. L. and A. P. Annan. 1989. Ground-penetrating radar for high-resolution mapping of soil and rock stratigraphy. *Geophysical Prospecting* 37: 531-551.
- Doolittle, J. A. 1987. Using ground-penetrating radar to increase the quality and efficiency of soil surveys. 11-32 pp. In: Reybold, W. U. and G. W. Peterson (eds.) *Soil Survey Techniques*, Soil Science Society of America. Special Publication No. 20. 98 p.
- Doolittle, J. A., R. A. Rebertus, G. B. Jordan, E. I. Swenson, and W. H. Taylor. 1988. Improving soil-landscape models by systematic sampling with ground-penetrating radar. *Soil Survey Horizons*. 29(2):46-54.
- Holloway, A. L. and J. C. Mugford. 1990. Fracture characterization in granite using ground probing radar. *CIM Bulletin* 83(940):61-70.
- Jones, D. P. and R. C. Graham. 1993. Water-holding characteristics of weathered granitic rock in chaparral and forest ecosystems. *Soil Science Society of America J.* 57:256-261.
- Leggo, P. J., J. M. Glover, and M. R. Wajzer. 1992. The detection and mapping of kaolinitic clay by ground probing radar in the Cornish granites of southwest England. pp. 205-215. IN: P. Hanninen and S. Autio (eds.) *Fourth International Conference on Ground-Penetrating Radar*. 7 to 12 June 1992. Rovaniemi, Finland. Geological Survey of Finland, Special Paper 16. pp. 365.
- Morey, R. M. 1974. Continuous subsurface profiling by impulse radar. p. 212-232. IN: *Proceedings, ASCE Engineering Foundation Conference on Subsurface Exploration for Underground Excavations and Heavy Construction*, held at Henniker, New Hampshire. Aug. 11-16, 1974.

- Olson, C. G. and J. A. Doolittle. 1985. Geophysical techniques for reconnaissance investigations of soils and surficial deposits in mountainous terrain. *Soil Sci. Soc. Am. J.* 49: 1490-1498.
- Puckett, W. E., M. E. Collins, and G. W. Schellentrager. 1990. Design of soil map units on a karst area in West Central Florida. *Soil Science Society of America J.* 54:1068-1073.
- Robillard, C. P. Nicolas, P. Armirat, M. Gariépy, and F. Goupil. 1994. Shallow Bedrock profiling using GPR. p. 1167-1179. IN: GPR 94. Proceedings of the Fifth International Conference on Ground Penetrating Radar. 12 to 16 June 1994. Kitchener, Ontario, Canada. Waterloo Center for Groundwater Research. pp. 1294.
- Rubin, L. A. and J. C. Fowler. 1978. Ground-probing radar for delineation of rock features. *Engineering Geology* 12: 163-170.
- Schellentrager, G. W. and J. A. Doolittle. 1991. Systematic sampling using ground-penetrating radar to study regional variation of a soil map unit. Chapter 12. p. 199-214. IN: Mausbach, M. J., and L. P. Wilding (eds.). *Spatial Variabilities of Soils and Landforms*. Soil Science Society of America Special Publication No. 28. pp. 270.
- Sigurdsson, T. 1994. Application of GPR for geological mapping, exploration of industrial mineralization and sulphide deposits p. 941-955. IN: GPR 94. Proceedings of the Fifth International Conference on Ground Penetrating Radar. 12 to 16 June 1994. Kitchener, Ontario, Canada. Waterloo Center for Groundwater Research. pp. 1294.
- Stevens, K. M., G. S. Lodha, A. L. Holloway, and N. M. Soonawala. 1995. The application of ground-penetrating radar for mapping fractures in plutonic rocks within the Whiteshell Research Area, Pinawa, Manitoba, Canada. *Journal of Applied Geophysics*. 33:125-141.

File 13

| <u>Scale</u> | <u>time</u> | <u>depth</u> |
|--------------|-------------|--------------|
| 36 | 70.2 | 6.2 |
| 34 | 66.3 | 5.9 |
| 30 | 58.5 | 5.2 |
| 26 | 50.7 | 4.5 |
| 25 | 48.8 | 4.4 |
| 26 | 50.7 | 4.5 |
| 27 | 52.7 | 4.7 |
| 23 | 44.9 | 4.0 |
| 20 | 39.0 | 3.5 |
| 17 | 33.2 | 3.0 |
| 20 | 39.0 | 3.5 |
| 19 | 37.1 | 3.3 |
| 18 | 35.1 | 3.2 |
| 18 | 35.1 | 3.2 |
| 24 | 46.8 | 4.2 |
| 22 | 42.9 | 3.8 |
| 25 | 48.8 | 4.4 |
| 30 | 58.5 | 5.2 |
| 33 | 64.4 | 5.7 |
| 34 | 66.3 | 5.9 |
| 36 | 70.2 | 6.2 |
| 37 | 72.2 | 6.4 |
| 37 | 72.2 | 6.4 |
| AVG: 4.7 | | |

File 14

| <u>Scale</u> | <u>time</u> | <u>depth</u> |
|--------------|-------------|--------------|
| 18 | 35.1 | 3.2 |
| 17 | 33.2 | 3.0 |
| 14 | 27.3 | 2.5 |
| 16 | 31.2 | 2.8 |
| 18 | 35.1 | 3.2 |
| 16 | 31.2 | 2.8 |
| 15 | 29.3 | 2.6 |
| 17 | 33.2 | 3.0 |
| 22 | 42.9 | 3.8 |
| 19 | 37.1 | 3.3 |
| 20 | 39.0 | 3.5 |
| 24 | 46.8 | 4.2 |
| 20 | 39.0 | 3.5 |
| 19 | 37.1 | 3.3 |
| 14 | 27.3 | 2.5 |
| 18 | 35.1 | 3.2 |
| 25 | 48.8 | 4.4 |
| 24 | 46.8 | 4.2 |
| 25 | 48.8 | 4.4 |
| 24 | 46.8 | 4.2 |
| 17 | 33.2 | 3.0 |
| 19 | 37.1 | 3.3 |
| 15 | 29.3 | 2.6 |
| 15 | 29.3 | 2.6 |
| 16 | 31.2 | 2.8 |
| 17 | 33.2 | 3.0 |
| AVG: 3.3 | | |

File 15

| <u>Scale</u> | <u>time</u> | <u>depth</u> |
|--------------|-------------|--------------|
| 16 | 31.2 | 2.8 |
| 16.5 | 32.2 | 2.9 |
| 14 | 27.3 | 2.5 |
| 17 | 33.2 | 3.0 |
| 12 | 23.4 | 2.1 |
| 8 | 15.6 | 1.4 |
| 19 | 37.1 | 3.3 |
| 12 | 23.4 | 2.1 |
| 13 | 25.4 | 2.3 |
| 10 | 19.5 | 1.8 |
| 8 | 15.6 | 1.4 |
| 16 | 31.2 | 2.8 |
| AVG: 2.4 | | |

File 16

| <u>Scale</u> | <u>time</u> | <u>depth</u> |
|--------------|-------------|--------------|
| 12 | 23.4 | 2.1 |
| 14 | 27.3 | 2.5 |
| 17 | 33.2 | 3.0 |
| 18 | 35.1 | 3.2 |
| 13 | 25.4 | 2.3 |
| 13 | 25.4 | 2.3 |
| 15 | 29.3 | 2.6 |
| 14 | 27.3 | 2.5 |
| 16 | 31.2 | 2.8 |
| 19 | 37.1 | 3.3 |
| 19 | 37.1 | 3.3 |
| 18 | 35.1 | 3.2 |
| 19 | 37.1 | 3.3 |
| 18 | 35.1 | 3.2 |
| 16 | 31.2 | 2.8 |
| 12 | 23.4 | 2.1 |
| 9 | 17.6 | 1.6 |
| 8 | 15.6 | 1.4 |
| 11 | 21.5 | 1.9 |
| 17 | 33.2 | 3.0 |
| 11 | 21.5 | 1.9 |
| 14 | 27.3 | 2.5 |
| 14 | 27.3 | 2.5 |
| AVG: 2.6 | | |

File 17

| <u>Scale</u> | <u>time</u> | <u>depth</u> |
|--------------|-------------|--------------|
| 24 | 46.8 | 4.2 |
| 19 | 37.1 | 3.3 |
| 16 | 31.2 | 2.8 |
| 13 | 25.4 | 2.3 |
| 12 | 23.4 | 2.1 |
| 16 | 31.2 | 2.8 |
| 22 | 42.9 | 3.8 |
| 18 | 35.1 | 3.2 |
| 14 | 27.3 | 2.5 |

File 17

| <u>Scale</u> | <u>time</u> | <u>depth</u> |
|--------------|-------------|--------------|
| 11 | 21.5 | 1.9 |
| 12 | 23.4 | 2.1 |
| 17 | 33.2 | 3.0 |
| 23 | 44.9 | 4.0 |
| 22 | 42.9 | 3.8 |
| 17 | 33.2 | 3.0 |
| 16 | 31.2 | 2.8 |
| 17 | 33.2 | 3.0 |
| 15 | 29.3 | 2.6 |
| 13 | 25.4 | 2.3 |
| 13 | 25.4 | 2.3 |
| 11 | 21.5 | 1.9 |
| 8 | 15.6 | 1.4 |
| 14 | 27.3 | 2.5 |
| 11 | 21.5 | 1.9 |
| 12 | 23.4 | 2.1 |
| 17 | 33.2 | 3.0 |
| AVG: 2.7 | | |

File 18

| <u>Scale</u> | <u>time</u> | <u>depth</u> |
|--------------|-------------|--------------|
| 15 | 22.0 | 2.0 |
| 14 | 20.5 | 1.9 |
| 13 | 19.0 | 1.7 |
| 17 | 24.9 | 2.2 |
| 20 | 29.3 | 2.6 |
| 21 | 30.7 | 2.8 |
| 22 | 32.2 | 2.9 |
| 20 | 29.3 | 2.6 |
| 23 | 33.7 | 3.0 |
| 18 | 26.3 | 2.4 |
| 19 | 27.8 | 2.5 |
| 24 | 35.1 | 3.2 |
| 21 | 30.7 | 2.8 |
| 16 | 23.4 | 2.1 |
| 14 | 20.5 | 1.9 |
| 12 | 17.6 | 1.6 |
| 12 | 17.6 | 1.6 |
| 13 | 19.0 | 1.7 |
| 14 | 20.5 | 1.9 |
| 13 | 19.0 | 1.7 |
| 12 | 17.6 | 1.6 |
| 18 | 26.3 | 2.4 |
| 21 | 30.7 | 2.8 |
| AVG: 2.3 | | |

File 19

| <u>Scale</u> | <u>time</u> | <u>depth</u> |
|--------------|-------------|--------------|
| 28 | 41.0 | 3.7 |
| 27 | 39.5 | 3.5 |
| 25 | 36.6 | 3.3 |
| 28 | 41.0 | 3.7 |
| 25 | 36.6 | 3.3 |
| 24 | 35.1 | 3.2 |
| 24 | 35.1 | 3.2 |
| 30 | 43.9 | 3.9 |
| 27 | 39.5 | 3.5 |
| 26 | 38.0 | 3.4 |
| 33 | 48.3 | 4.3 |
| 33 | 48.3 | 4.3 |
| 32 | 46.8 | 4.2 |
| 30 | 43.9 | 3.9 |
| 25 | 36.6 | 3.3 |
| 28 | 41.0 | 3.7 |
| | AVG: | 3.6 |

File 20

| <u>Scale</u> | <u>time</u> | <u>depth</u> |
|--------------|-------------|--------------|
| 14 | 20.5 | 1.9 |
| 14 | 20.5 | 1.9 |
| 15 | 22.0 | 2.0 |
| 12 | 17.6 | 1.6 |
| 14 | 20.5 | 1.9 |
| 21 | 30.7 | 2.8 |
| 33 | 48.3 | 4.3 |
| 31 | 45.4 | 4.1 |
| 23 | 33.7 | 3.0 |
| 18 | 26.3 | 2.4 |
| 26 | 38.0 | 3.4 |
| 34 | 49.8 | 4.4 |
| 33 | 48.3 | 4.3 |
| 27 | 39.5 | 3.5 |
| 24 | 35.1 | 3.2 |
| 27 | 39.5 | 3.5 |
| 22 | 32.2 | 2.9 |
| 24 | 35.1 | 3.2 |
| 34 | 49.8 | 4.4 |
| 41 | 60.0 | 5.3 |
| 29 | 42.4 | 3.8 |
| 17 | 24.9 | 2.2 |
| 17 | 24.9 | 2.2 |
| 18 | 26.3 | 2.4 |
| 17 | 24.9 | 2.2 |
| 17 | 24.9 | 2.2 |
| 14 | 20.5 | 1.9 |
| | AVG: | 3.0 |

File 21

| <u>Scale</u> | <u>time</u> | <u>depth</u> |
|--------------|-------------|--------------|
| 39 | 57.1 | 5.1 |
| 31 | 45.4 | 4.1 |
| 23 | 33.7 | 3.0 |
| 28 | 41.0 | 3.7 |

File 21

| <u>Scale</u> | <u>time</u> | <u>depth</u> |
|--------------|-------------|--------------|
| 29 | 42.4 | 3.8 |
| 27 | 39.5 | 3.5 |
| 31 | 45.4 | 4.1 |
| 32 | 46.8 | 4.2 |
| 36 | 52.7 | 4.7 |
| 36 | 52.7 | 4.7 |
| 36 | 52.7 | 4.7 |
| 30 | 43.9 | 3.9 |
| 29 | 42.4 | 3.8 |
| 30 | 43.9 | 3.9 |
| 30 | 43.9 | 3.9 |
| 34 | 49.8 | 4.4 |
| 37 | 54.1 | 4.8 |
| 38 | 55.6 | 5.0 |
| 38 | 55.6 | 5.0 |
| 31 | 45.4 | 4.1 |
| 33 | 48.3 | 4.3 |
| 35 | 51.2 | 4.6 |
| 37 | 54.1 | 4.8 |
| 61 | 89.3 | 7.9 |
| 58 | 84.9 | 7.5 |
| 49 | 71.7 | 6.4 |
| 32 | 46.8 | 4.2 |
| 27 | 39.5 | 3.5 |
| 35 | 51.2 | 4.6 |
| | AVG: | 4.6 |

File 22

| <u>Scale</u> | <u>time</u> | <u>depth</u> |
|--------------|-------------|--------------|
| 35 | 51.2 | 4.6 |
| 33 | 48.3 | 4.3 |
| 27 | 39.5 | 3.5 |
| 25 | 36.6 | 3.3 |
| 31 | 45.4 | 4.1 |
| 43 | 62.9 | 5.6 |
| 50 | 73.2 | 6.5 |
| 53 | 77.6 | 6.9 |
| 54 | 79.0 | 7.0 |
| 62 | 90.7 | 8.0 |
| 64 | 93.7 | 8.3 |
| 62 | 90.7 | 8.0 |
| 45 | 65.9 | 5.9 |
| 38 | 55.6 | 5.0 |
| 27 | 39.5 | 3.5 |
| 31 | 45.4 | 4.1 |
| 27 | 39.5 | 3.5 |
| 23 | 33.7 | 3.0 |
| | AVG: | 5.3 |

File 23

| <u>Scale</u> | <u>time</u> | <u>depth</u> |
|--------------|-------------|--------------|
| 21 | 30.7 | 2.8 |
| 13 | 19.0 | 1.7 |
| 18 | 26.3 | 2.4 |
| 22 | 32.2 | 2.9 |
| 17 | 24.9 | 2.2 |

File 23

| <u>Scale</u> | <u>time</u> | <u>depth</u> |
|--------------|-------------|--------------|
| 15 | 22.0 | 2.0 |
| 17 | 24.9 | 2.2 |
| 17 | 24.9 | 2.2 |
| 16 | 23.4 | 2.1 |
| 11 | 16.1 | 1.5 |
| 8 | 11.7 | 1.1 |
| 8 | 11.7 | 1.1 |
| 8 | 11.7 | 1.1 |
| 8 | 11.7 | 1.1 |
| 10 | 14.6 | 1.3 |
| 11 | 16.1 | 1.5 |
| 11 | 16.1 | 1.5 |
| 11 | 16.1 | 1.5 |
| 13 | 19.0 | 1.7 |
| 14 | 20.5 | 1.9 |
| 13 | 19.0 | 1.7 |
| 12 | 17.6 | 1.6 |
| 9 | 13.2 | 1.2 |
| 14 | 20.5 | 1.9 |
| 15 | 22.0 | 2.0 |
| 15 | 22.0 | 2.0 |
| | AVG: | 1.8 |

File 24

| <u>Scale</u> | <u>time</u> | <u>depth</u> |
|--------------|-------------|--------------|
| 15 | 22.0 | 2.0 |
| 24 | 35.1 | 3.2 |
| 34 | 49.8 | 4.4 |
| 42 | 61.5 | 5.5 |
| 60 | 87.8 | 7.8 |
| 69 | 101.0 | 8.9 |
| 75 | 109.8 | 9.7 |
| 61 | 89.3 | 7.9 |
| 68 | 99.5 | 8.8 |
| 55 | 80.5 | 7.1 |
| 48 | 70.2 | 6.2 |
| 39 | 57.1 | 5.1 |
| 35 | 51.2 | 4.6 |
| 35 | 51.2 | 4.6 |
| 35 | 51.2 | 4.6 |
| 36 | 52.7 | 4.7 |
| 37 | 54.1 | 4.8 |
| 35 | 51.2 | 4.6 |
| 35 | 51.2 | 4.6 |
| 33 | 48.3 | 4.3 |
| 27 | 39.5 | 3.5 |
| 20 | 29.3 | 2.6 |
| 19 | 27.8 | 2.5 |
| 17 | 24.9 | 2.2 |
| 15 | 22.0 | 2.0 |
| 15 | 22.0 | 2.0 |
| 14 | 20.5 | 1.9 |
| 14 | 20.5 | 1.9 |
| 16 | 23.4 | 2.1 |
| | AVG: | 4.6 |

File 25

| <u>Scale</u> | <u>time</u> | <u>depth</u> |
|--------------|-------------|--------------|
| 19 | 27.8 | 2.5 |
| 29 | 42.4 | 3.8 |
| 33 | 48.3 | 4.3 |
| 31 | 45.4 | 4.1 |
| 27 | 39.5 | 3.5 |
| 33 | 48.3 | 4.3 |
| 36 | 52.7 | 4.7 |
| 33 | 48.3 | 4.3 |
| 35 | 51.2 | 4.6 |
| 33 | 48.3 | 4.3 |
| 30 | 43.9 | 3.9 |
| 22 | 32.2 | 2.9 |
| 23 | 33.7 | 3.0 |
| 27 | 39.5 | 3.5 |
| 21 | 30.7 | 2.8 |
| 20 | 29.3 | 2.6 |
| 15 | 22.0 | 2.0 |
| 9 | 13.2 | 1.2 |
| 10 | 14.6 | 1.3 |
| 29 | 42.4 | 3.8 |
| 28 | 41.0 | 3.7 |
| 27 | 39.5 | 3.5 |
| 23 | 33.7 | 3.0 |
| 20 | 29.3 | 2.6 |
| 16 | 23.4 | 2.1 |
| 16 | 23.4 | 2.1 |
| 16 | 23.4 | 2.1 |
| 15 | 22.0 | 2.0 |
| 14 | 20.5 | 1.9 |
| 13 | 19.0 | 1.7 |
| 18 | 26.3 | 2.4 |
| | AVG: | 3.1 |

File26

| <u>Scale</u> | <u>time</u> | <u>depth</u> |
|--------------|-------------|--------------|
| 23 | 33.7 | 3.0 |
| 22 | 32.2 | 2.9 |
| 20 | 29.3 | 2.6 |
| 21 | 30.7 | 2.8 |
| 20 | 29.3 | 2.6 |
| 23 | 33.7 | 3.0 |
| 22 | 32.2 | 2.9 |
| 24 | 35.1 | 3.2 |
| 24 | 35.1 | 3.2 |
| 17 | 24.9 | 2.2 |
| 16 | 23.4 | 2.1 |
| 21 | 30.7 | 2.8 |
| 22 | 32.2 | 2.9 |
| 18 | 26.3 | 2.4 |
| 13 | 19.0 | 1.7 |
| 16 | 23.4 | 2.1 |
| 20 | 29.3 | 2.6 |
| 20 | 29.3 | 2.6 |
| 19 | 27.8 | 2.5 |
| 17 | 24.9 | 2.2 |

File26

| <u>Scale</u> | <u>time</u> | <u>depth</u> |
|--------------|-------------|--------------|
| 15 | 22.0 | 2.0 |
| 18 | 26.3 | 2.4 |
| 15 | 22.0 | 2.0 |
| 14 | 20.5 | 1.9 |
| 17 | 24.9 | 2.2 |
| 14 | 20.5 | 1.9 |
| 15 | 22.0 | 2.0 |
| | AVG: | 2.5 |

File27

| <u>Scale</u> | <u>time</u> | <u>depth</u> |
|--------------|-------------|--------------|
| 20 | 29.3 | 2.6 |
| 15 | 22.0 | 2.0 |
| 15 | 22.0 | 2.0 |
| 13 | 19.0 | 1.7 |
| 18 | 26.3 | 2.4 |
| 15 | 22.0 | 2.0 |
| 15 | 22.0 | 2.0 |
| 14 | 20.5 | 1.9 |
| 17 | 24.9 | 2.2 |
| 16 | 23.4 | 2.1 |
| 14 | 20.5 | 1.9 |
| 15 | 22.0 | 2.0 |
| 18 | 26.3 | 2.4 |
| 24 | 35.1 | 3.2 |
| 24 | 35.1 | 3.2 |
| 25 | 36.6 | 3.3 |
| 20 | 29.3 | 2.6 |
| 19 | 27.8 | 2.5 |
| 21 | 30.7 | 2.8 |
| 17 | 24.9 | 2.2 |
| 17 | 24.9 | 2.2 |
| 16 | 23.4 | 2.1 |
| 17 | 24.9 | 2.2 |
| 18 | 26.3 | 2.4 |
| 20 | 29.3 | 2.6 |
| 20 | 29.3 | 2.6 |
| 17 | 24.9 | 2.2 |
| 13 | 19.0 | 1.7 |
| 12 | 17.6 | 1.6 |
| 12 | 17.6 | 1.6 |
| 14 | 20.5 | 1.9 |
| | AVG: | 2.3 |

File28

| <u>Scale</u> | <u>time</u> | <u>depth</u> |
|--------------|-------------|--------------|
| 21 | 30.7 | 2.8 |
| 19 | 27.8 | 2.5 |
| 17 | 24.9 | 2.2 |
| 10 | 14.6 | 1.3 |
| 14 | 20.5 | 1.9 |
| 13 | 19.0 | 1.7 |
| 24 | 35.1 | 3.2 |
| 12 | 17.6 | 1.6 |
| 12 | 17.6 | 1.6 |
| 17 | 24.9 | 2.2 |

File28

| <u>Scale</u> | <u>time</u> | <u>depth</u> |
|--------------|-------------|--------------|
| 18 | 26.3 | 2.4 |
| 19 | 27.8 | 2.5 |
| 20 | 29.3 | 2.6 |
| 20 | 29.3 | 2.6 |
| | AVG: | 2.2 |

File29

| <u>Scale</u> | <u>time</u> | <u>depth</u> |
|--------------|-------------|--------------|
| 20 | 29.3 | 2.6 |
| 16 | 23.4 | 2.1 |
| 17 | 24.9 | 2.2 |
| 12 | 17.6 | 1.6 |
| 13 | 19.0 | 1.7 |
| 14 | 20.5 | 1.9 |
| 16 | 23.4 | 2.1 |
| 17 | 24.9 | 2.2 |
| 19 | 27.8 | 2.5 |
| 13 | 19.0 | 1.7 |
| 12 | 17.6 | 1.6 |
| 14 | 20.5 | 1.9 |
| 18 | 26.3 | 2.4 |
| | AVG: | 2.1 |

File30

| <u>Scale</u> | <u>time</u> | <u>depth</u> |
|--------------|-------------|--------------|
| 10 | 14.6 | 1.3 |
| 10 | 14.6 | 1.3 |
| 14 | 20.5 | 1.9 |
| 15 | 22.0 | 2.0 |
| 16 | 23.4 | 2.1 |
| 16 | 23.4 | 2.1 |
| 17 | 24.9 | 2.2 |
| 14 | 20.5 | 1.9 |
| 13 | 19.0 | 1.7 |
| 10 | 14.6 | 1.3 |
| | AVG: | 1.8 |

File31

| <u>Scale</u> | <u>time</u> | <u>depth</u> |
|--------------|-------------|--------------|
| 24 | 35.1 | 3.2 |
| 26 | 38.0 | 3.4 |
| 30 | 43.9 | 3.9 |
| 40 | 58.5 | 5.2 |
| 46 | 67.3 | 6.0 |
| 46 | 67.3 | 6.0 |
| 59 | 86.3 | 7.7 |
| 57 | 83.4 | 7.4 |
| 46 | 67.3 | 6.0 |
| 50 | 73.2 | 6.5 |
| 44 | 64.4 | 5.7 |
| 37 | 54.1 | 4.8 |
| 30 | 43.9 | 3.9 |
| 24 | 35.1 | 3.2 |
| 18 | 26.3 | 2.4 |
| 17 | 24.9 | 2.2 |
| 18 | 26.3 | 2.4 |

File31

| <u>Scale</u> | <u>time</u> | <u>depth</u> |
|--------------|-------------|--------------|
| 22 | 32.2 | 2.9 |
| 26 | 38.0 | 3.4 |
| 30 | 43.9 | 3.9 |
| 34 | 49.8 | 4.4 |
| 45 | 65.9 | 5.9 |
| 51 | 74.6 | 6.6 |
| 45 | 65.9 | 5.9 |
| 41 | 60.0 | 5.3 |
| 34 | 49.8 | 4.4 |
| 30 | 43.9 | 3.9 |
| | AVG: | 4.7 |

File33

| <u>Scale</u> | <u>time</u> | <u>depth</u> |
|--------------|-------------|--------------|
| 26 | 50.7 | 4.5 |
| 24 | 46.8 | 4.2 |
| 25 | 48.8 | 4.4 |
| 27 | 52.7 | 4.7 |
| 29 | 56.6 | 5.0 |
| 32 | 62.4 | 5.6 |
| 32 | 62.4 | 5.6 |
| 34 | 66.3 | 5.9 |
| 37 | 72.2 | 6.4 |
| 35 | 68.3 | 6.1 |
| 37 | 72.2 | 6.4 |
| 37 | 72.2 | 6.4 |
| 33 | 64.4 | 5.7 |
| 29 | 56.6 | 5.0 |
| 27 | 52.7 | 4.7 |
| 25 | 48.8 | 4.4 |
| 28 | 54.6 | 4.9 |
| 28 | 54.6 | 4.9 |
| 22 | 42.9 | 3.8 |

File33

| <u>Scale</u> | <u>time</u> | <u>depth</u> |
|--------------|-------------|--------------|
| 20 | 39.0 | 3.5 |
| 17 | 33.2 | 3.0 |
| 16 | 31.2 | 2.8 |
| 22 | 42.9 | 3.8 |
| | AVG: | 4.9 |

File34

| <u>Scale</u> | <u>time</u> | <u>depth</u> |
|--------------|-------------|--------------|
| 17 | 33.2 | 3.0 |
| 23 | 44.9 | 4.0 |
| 27 | 52.7 | 4.7 |
| 29 | 56.6 | 5.0 |
| 30 | 58.5 | 5.2 |
| 20 | 39.0 | 3.5 |
| 16 | 31.2 | 2.8 |
| 28 | 54.6 | 4.9 |
| 31 | 60.5 | 5.4 |
| 31 | 60.5 | 5.4 |
| 30 | 58.5 | 5.2 |
| 27 | 52.7 | 4.7 |
| 28 | 54.6 | 4.9 |
| 33 | 64.4 | 5.7 |
| 31 | 60.5 | 5.4 |
| 30 | 58.5 | 5.2 |
| 25 | 48.8 | 4.4 |
| 20 | 39.0 | 3.5 |
| 18 | 35.1 | 3.2 |
| 16 | 31.2 | 2.8 |
| 19 | 37.1 | 3.3 |
| 20 | 39.0 | 3.5 |
| 20 | 39.0 | 3.5 |
| 25 | 48.8 | 4.4 |
| 26 | 50.7 | 4.5 |
| 28 | 54.6 | 4.9 |

File34

| <u>Scale</u> | <u>time</u> | <u>depth</u> |
|--------------|-------------|--------------|
| 17 | 33.2 | 3.0 |
| 15 | 29.3 | 2.6 |
| 16 | 31.2 | 2.8 |
| 19 | 37.1 | 3.3 |
| 20 | 39.0 | 3.5 |
| | AVG: | 4.1 |

File35

| <u>Scale</u> | <u>time</u> | <u>depth</u> |
|--------------|-------------|--------------|
| 15 | 29.3 | 2.6 |
| 25 | 48.8 | 4.4 |
| 28 | 54.6 | 4.9 |
| 31 | 60.5 | 5.4 |
| 28 | 54.6 | 4.9 |
| 38 | 74.1 | 6.6 |
| 34 | 66.3 | 5.9 |
| 22 | 42.9 | 3.8 |
| 14 | 27.3 | 2.5 |
| 15 | 29.3 | 2.6 |
| 20 | 39.0 | 3.5 |
| 23 | 44.9 | 4.0 |
| 14 | 27.3 | 2.5 |
| 15 | 29.3 | 2.6 |
| 13 | 25.4 | 2.3 |
| 16 | 31.2 | 2.8 |
| 17 | 33.2 | 3.0 |
| 16 | 31.2 | 2.8 |
| 13 | 25.4 | 2.3 |
| 14 | 27.3 | 2.5 |
| 16 | 31.2 | 2.8 |
| 19 | 37.1 | 3.3 |
| 16 | 31.2 | 2.8 |
| 16 | 31.2 | 2.8 |
| | AVG: | 3.5 |